Surface Chemistry

DOI: 10.1002/ange.201107668

Unique Electrochemical Adsorption Properties of Pt-Skin Surfaces**

*Dennis F. van der Vliet, Chao Wang, Dongguo Li, Arvydas P. Paulikas, Jeffrey Greeley, Rees B. Rankin, Dusan Strmcnik, Dusan Tripkovic, Nenad M. Markovic, and Vojislav R. Stamenkovic**

PtM alloys (M = Co, Ni, Fe, etc.) have been extensively studied for their use in fuel cells, both in well-defined extended surfaces,[1] as well as in nanoparticles.[2] After the report about exceptional activity of $Pt_3Ni(111)$-skin surface[1a] for the oxygen reduction reaction (ORR) a lot of efforts have been made to mimic this catalytic behavior at the nanoscale. It has been shown that a $Pt_3Ni(111)$ crystal annealed in ultra-high vacuum (UHV) shows an oscillating segregation profile, with the outermost layer consisting of pure platinum while the second layer is enriched in nickel compared to the bulk composition.[1a,3] Such a surface we termed Pt skin, and owing to the presence of the non-noble metal in the subsurface layer it has altered electronic properties compared to the mono-metallic Pt single crystal with the same orientation. Accordingly, altered electronic properties induce a change in adsorption behavior, specifically a shift of surface-oxide formation to higher potentials.[1a,b] This adsorption behavior is believed to be the origin of the high activity for the ORR. On the opposite side of the potential scale, the adsorption of hydrogenated species, denoted as underpotentially adsorbed hydrogen (H_{upd}), is also largely affected on Pt-skin surfaces.[4] Despite numerous efforts dedicated to synthesize nanocatalysts with Pt-skin-type surfaces,[2c,5] it still remains a challenge to claim their existence at the nanoscale. To systematically resolve this issue, we attempt to provide fundamental insight into the adsorption properties of well-defined Pt-skin surfaces under relevant electrochemical conditions and to transfer that knowledge to corresponding nanocatalysts.

For that reason, we first examine the formation and composition of Pt-skin surfaces by low-energy ion scattering (LEIS) and scanning tunneling microscopy (STM) in UHV, and second we study the composition of the surfaces in an electrochemical environment to establish their adsorption properties. We demonstrate by cyclic voltammetry that the surface coverage of H_{upd} on Pt skin is about half of that found on Pt(111), whereas the surface coverage of a saturated monolayer of carbon monoxide is similar for both surfaces. This is an important finding, which provides a link towards accurate determination of the electrochemically active surface area of nanoscale catalysts. The developed methodology provides additional evidence for the existence of Pt-skin surfaces on Pt-bimetallic nanocatalysts and can substantially diminish errors in the evaluation of the real surface area and catalytic activity.

A thorough examination of the Pt-skin surfaces was performed in view of their importance in electrocatalysis as well as in response to recent questions and doubts in the

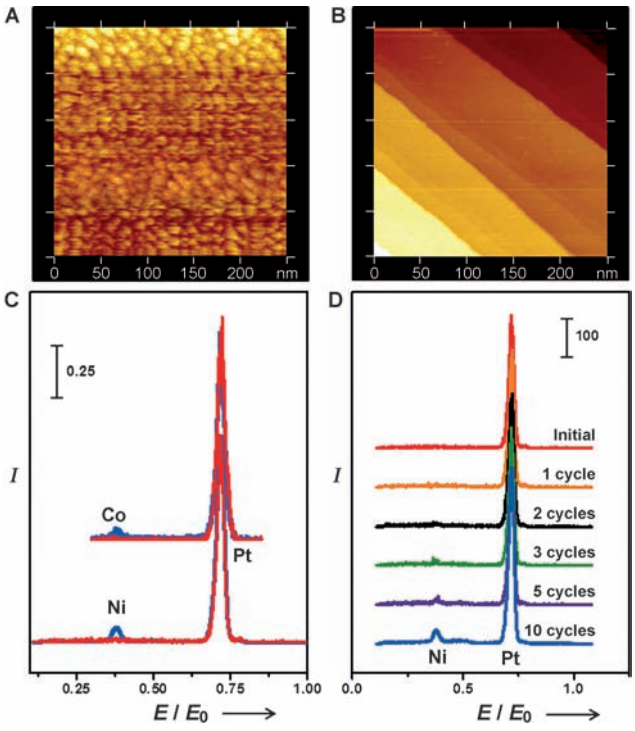

Figure 1. Surface characterization of $Pt_3M(111)$ surfaces in UHV: STM images of A) sputtered and B) annealed $Pt_3Ni(111)$ surfaces. The brightness in colors is a measure of the depth profile, with each color change marking a single atomic step. Low-energy ion scattering spectra of C) sputtered (blue traces) versus annealed (red traces) surfaces of $Pt_3Ni(111)$ and $Pt_3Co(111)$ crystals. D) Successive LEIS spectra of $Pt_3Ni(111)$ surface during Ne-sputtering. The graphs in (C) and (D) are shifted, and the scale bars indicate the intensities in arbitrary units. E/E_0 is the ratio of the energy of the scattered ion beam (E) and the energy of the incident ion beam (E_0).

[*] Dr. D. F. van der Vliet, Dr. C. Wang, D. Li, A. P. Paulikas, Dr. D. Strmcnik, Dr. D. Tripkovic, Dr. N. M. Markovic, Dr. V. R. Stamenkovic
Materials Science Division, Argonne National Lab
9700 S. Cass Ave, Argonne IL (USA)
E-mail: vrstamenkovic@anl.gov
vrstamenkovic@anl.gov

D. Li
Brown University
1 Prospect St., Providence, RI, 12912, USA

Dr. J. Greeley, Dr. R. B. Rankin
Center for Nanoscale Materials, Argonne National Lab
9700 S. Cass Ave, Argonne IL (USA)

[**] This work was supported by the U.S. Department of Energy, Office of Science, Office of Basic Energy Sciences, under contract No. DE-AC02-06CH11357.

Supporting information for this article is available on the WWW under http://dx.doi.org/10.1002/anie.201107668.

literature[6] on if the state of the Pt-skin surface formed over the Pt_3M systems in UHV and in an electrochemical environment consists of pure Pt. Figure 1C shows the LEIS results obtained by a 1 keV Ne^+ ion beam for the $Pt_3Ni(111)$ and $Pt_3Co(111)$ crystals before and after thermal annealing in UHV. Based on these LEIS spectra it is obvious that after consecutive annealing/sputtering cycles, both Pt and Ni (or Co) are present on the surface, while the STM image in Figure 1A illustrates the roughness of the sputtered surface. However, the LEIS signal for Ni and/or Co is diminished if annealing is the final step, which is indicative for the formation of a Pt skin. The morphology of this surface is revealed by STM (Figure 1B), which displays the smooth and ordered formation that is typical for single-crystalline systems. To investigate the stability of these surfaces in UHV, more energy was applied through the monochromatic Ne^+ ion beam, causing a sputtering effect to take place on the topmost Pt surface layer. Consequently, the subsurface nickel and/or cobalt atoms become exposed in consecutive LEIS spectra (shown for $Pt_3Ni(111)$ in Figure 1D; the result for $Pt_3Co(111)$ was identical), indicating a change in surface composition from Pt-skin (100% Pt) into Pt-rich. These combined LEIS and STM results unambiguously confirm that both crystals exhibit substantial transition of surface composition/morphology upon annealing in UHV owing to complete segregation of Pt to the surface, thereby forming a full Pt skin.

Cyclic voltammetry is used to examine electrochemical adsorption properties of Pt-skin surfaces.[9] As shown in Figure 2A, the onset of H_{upd} adsorption on $Pt_3Ni(111)$ skin is shifted towards lower potentials when compared to Pt(111). The onset is approximately 150 mV lower and shows a reversible pre-wave ahead of the main H_{upd} adsorption owing to surface steps, which are inevitably present on $Pt_3Ni(111)$. Moreover, the formation of surface oxides OH_{ad} at potentials greater than 0.6 V is delayed by 100 mV versus Pt(111).[1a] Furthermore, from the integrated H_{upd} regions it was revealed that charges are considerably different (see Table 1), i.e., in the same potential range, Pt-skin surfaces have about half of the value obtained for Pt(111).

It is important to emphasize that Pt(111) and $Pt_3M(111)$-skin surfaces have essentially identical geometric surface areas, surface compositions, and surface structures, albeit the interatomic distances may be altered by the composition of the second layer. However, the electrochemical adsorption properties between them are quite different. This is a consequence of the electronically modified structure of Pt for Pt-skin surfaces by Ni or Co subsurface atoms, which leads to weakened interactions between Pt and adsorbates such as H_{upd} and OH_{ad}. The H_{upd} integrated charge is used as conventional approach in the estimation of the electrochemical surface area; however, the discrepancy that is coming from altered electronic properties of Pt can substantially affect the accurate estimation of the real surface area of Pt-alloy catalysts.

Table 1: Integrated charges for Pt(111), $Pt_3Ni(111)$, Pt_3Co (111), and polycrystalline-Pt (Pt(poly)) extended surfaces obtained from cyclic voltammetry curves for H_{upd} (Q_H), CO stripping (Q_{CO}), and the ratio between measured charges. Analysis of the charges can be found in the Supporting Information.

Catalyst	Q_H [$\mu C\,cm^{-2}$]	Q_{CO} [$\mu C\,cm^{-2}$]	$Q_{CO}/2\,Q_H$
Pt(111)	152	315	1.04
$Pt_3Ni(111)$	98	304	1.55
$Pt_3Co(111)$	91	283	1.55
Pt(poly)	190	386	1.02

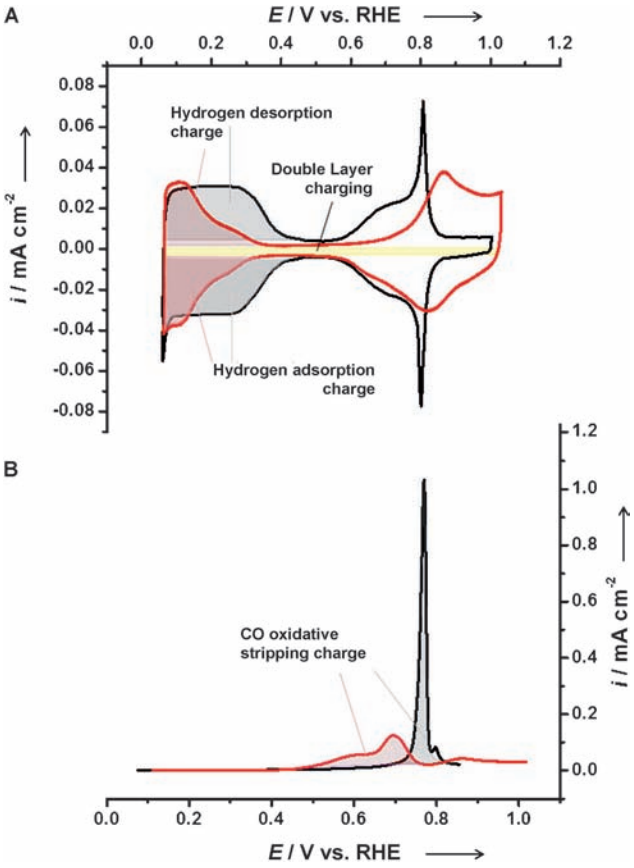

Figure 2. Electrochemical characterization of Pt(111) (black traces) and $Pt_3Ni(111)$-skin surfaces (red traces) by using a rotating disc electrode (RDE) in 0.1 M $HClO_4$: A) cyclic voltammograms; B) electro-oxidation of an adsorbed monolayer of CO on Pt(111) and on $Pt_3Ni(111)$ skin. RHE = reversible hydrogen electrode.

Another surface-sensitive reaction that is commonly used to probe surface properties is the electro-oxidation of adsorbed carbon monoxide, well-known as CO stripping. In this reaction, the surface is first saturated with a CO adlayer at the negative potential limit. Owing to a strong $Pt–CO_{ad}$ interaction, CO molecules stay adsorbed on Pt surface atoms, while the electrolyte is purged with argon gas. The consecutive step is electro-oxidation of CO by sweeping the potential towards the positive limit. The obtained CO stripping voltammetric profiles of surfaces prepared in UHV are shown in Figure 2B. The onset of CO stripping on $Pt_3Ni(111)$ skin is 150 mV lower than that on Pt(111), while the shape of the stripping peak is much broader, and the main oxidation peak is also shifted by about 100 mV. The oxidation of adsorbed CO_{ad} proceeds at lower potentials on Pt-skin surfaces owing to a weaker interaction of the Pt surface atoms with CO, caused by the modified electronic properties, but the

similar charge of CO oxidation points to an equal coverage of CO.[7] This hypothesis is supported by our density functional theory calculations, which indicate that CO binding to a $Pt_3Ni(111)$-skin surface, with a 1:1 Pt/Ni ratio in the subsurface layer, is approximately 0.27 eV weaker than the corresponding binding on Pt(111).[10] For that reason, the reduced binding of surface oxides (OH_{ad}) on Pt_3Ni (111) skin does not cause an increase in onset potential for CO electrooxidation. In fact, since CO_{ad} and OH_{ad} are competing for the same Pt adsorption sites, the reduced binding energy between Pt_3Ni (111) skin and CO_{ad} leads to a lower onset potential as the blocking effect of CO_{ad} is diminished (see the Supporting Information for additional computational details). It is important to mention that it was demonstrated that CO_{ad} can modify the surface composition and/or morphology;[8] such an effect would imply a stronger Pt–CO interaction, whereas we clearly note a weakened adsorption, convincingly disproving such an interaction in the Pt-skin case. This was additionally confirmed by unchanged cyclic voltammetry after CO electrooxidation.

Based on the results depicted in Figure 2 B and Table 1 the onset, shape, and main oxidation peak of the CO stripping curves differ between $Pt_3M(111)$-skin surfaces and Pt(111), while the integrated charges are nearly equal. The similar CO stripping charges add to the LEIS evidence that the outer layer of the $Pt_3M(111)$ skin consists of only Pt atoms. Moreover, the ratio between the charges of CO stripping versus H_{upd} was calculated to visualize the difference in adsorption properties for all surfaces (see Table 1). Both H_{upd} and CO stripping are surface-specific probes for Pt atoms, so in case of pure Pt systems, such as Pt(111) and polycrystalline Pt, this charge ratio is identical and close to one. However, the ratio obtained for $Pt_3Ni(111)$- and $Pt_3Co(111)$-skin surfaces is 1.55, which confirms that the surface coverage of CO_{ad} is not affected by altered electronic properties of Pt-skin surfaces. As a consequence of these results, it is obvious that the integrated H_{upd} region cannot be solely used in estimation of the electrochemical surface area in case of Pt-skin surfaces. For that reason, special care must be taken when analyzing annealed PtM alloys in the form of high-surface-area nanoscale catalysts.

As a case in point, in Table 2 the charges for H_{upd} and CO oxidation are compared for three different catalysts of equally sized nanoparticles (NPs): monometallic Pt/C, PtNi/C, and annealed PtNi/C NPs with a Pt skin. Detailed information on the particles' size distribution and composition is presented in the Supporting Information. Transmission electron microscopy (TEM) results show that the particles' size of about 5 nm and shape are not affected by thermal annealing, while energy-dispersive X-ray (EDX) line scan analyses revealed the elemental distribution across the particles. In Figure S1 in the Supporting Information, a uniform distribution of Pt and Ni is confirmed for as-prepared particles. On the other hand, after the acid leaching and annealing treatments, a Pt-overlayer has emerged on PtNi nanoparticles. Representative voltammetric curves for skin-type PtNi NPs compared to Pt/C can be seen in Figure 3. The CO stripping curves in Figure 3 B closely match the results obtained on single crystals (Figure 2 B). For the non-annealed NPs, the ratio between the

Table 2: Integrated charges and calculated surface areas (ECSAs) for H_{upd} (Q_H) and CO stripping (Q_{CO}) obtained from cyclic voltammetries of Pt/C, acid-treated PtNi/C, and annealed PtNi/C catalysts. The ratio between the integrated charges for H_{upd} and CO stripping demonstrates the discrepancy in ECSAs and the underestimation of the real surface area if H_{upd} is used in case of Pt-skin surfaces.

Catalyst	Q_H [μC]	$ECSA_H$ [cm^2]	Q_{CO} [μC]	$ECSA_{CO}$ [cm^2]	$Q_{CO}/2\,Q_H$
Pt/C	279	1.47	545	1.41	0.98
PtNi/C	292	1.54	615	1.60	1.05
PtNi skin/C	210	1.10	595	1.54	1.42

charges for H_{upd} and CO stripping is similar to Pt/C (and Pt(poly)), and thus the surface-area estimation based on the H_{upd} charge is reasonable. However, the adsorption properties of annealed PtNi particles with a Pt-skin-type surface resemble those previously established on well-defined skin-type bulk crystals of $Pt_3Ni(111)$ and $Pt_3Co(111)$, as judged by the suppression of H_{upd} adsorption (measured as charge).

This suppression of H_{upd} adsorption confirms that the current focus in nanoparticle research on skin-type or core–shell structures[2c,5] can potentially suffer from substantial underestimation of the electrochemically active surface area if only the integrated H_{upd} region is used. To be certain that the electrochemical surface area is not overlooked for skin-type alloy catalysts, the estimated H_{upd} charge always has to be

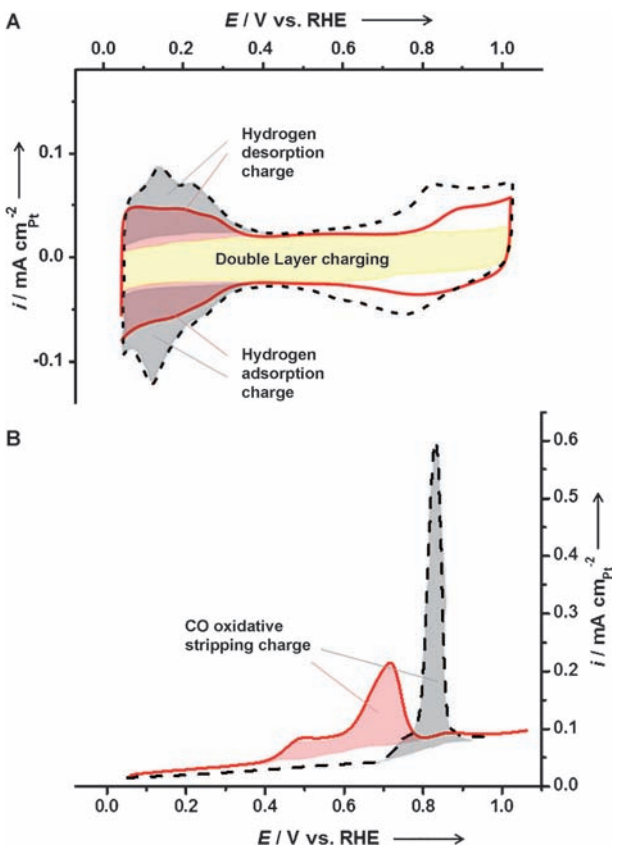

Figure 3. Electrochemical surface characterization of catalysts consisting of Pt/C (black dashed traces) and PtNi/C with Pt skin (red traces) by using a RDE in 0.1 M $HClO_4$: A) cyclic voltammograms; B) CO stripping curves.

compared to the CO stripping charge. Furthermore, the observed discrepancy between surface-area estimations based on H_{upd} and CO stripping can give an indication of the formation of a skin-type nanocatalyst alloy, because acid leached skeleton-type surfaces and nanoparticles do not show such behavior.

In summary, we have demonstrated that by alloying platinum with a non-noble second metal and inducing a Pt-skin-type structure, the adsorption properties of the resulting PtM alloys are significantly altered. Specifically, the adsorption of hydrogen and oxide species is shifted in potential and reduced in magnitude compared to monometallic Pt in the same potential region. Added to LEIS evidence, the fact that the charge of the oxidation of a complete monolayer of CO is similar on annealed Pt_3M surfaces as on monometallic Pt confirms the surface consists of only platinum. The suppression of H_{upd} adsorptionon these surfaces is both a method to confirm Pt-skin formation, but also prompts a difficulty in determining the electrochemically active surface area on Pt-skin-type nanoparticles. To avoid underestimation of the surface area owing to suppression of H_{upd} adsorption, and hence overrating of specific activity, we demonstrate that CO stripping has to be used alongside the H_{upd} charge for the determination of the electrochemically active surface area of Pt-alloy catalysts.

Experimental Section

Methods: After annealing cycles in UHV, the $Pt_3Ni(111)$ crystal was transferred to the electrochemical cell in hanging meniscus mode in which only the (111) surface is exposed to the electrolyte. The crystal was protected from the airborne impurities by a drop of hydrogen-saturated Milli-Q water during transfer to the electrolyte, which was deoxygenated 0.1 M $HClO_4$. All gases are of research grade (5N5 or higher).

After voltammetry confirmed a clean and stable surface, CO was inserted into the cell for one minute, while the crystal was rotated at 1600 rpm. Consecutively, rotation was stopped and argon was bubbled through the cell for 45 min to remove any trace of dissolved CO. After CO was purged from the solution, two cycles were recorded: the first one being the CO stripping voltammetry, the second to verify the absence of residual CO in solution. All electrochemical measurements were performed with a scan rate of 50 $mV\,s^{-1}$ in 0.1 M $HClO_4$ at room temperature.

The electrochemical glass cell was a standard 3-electrode cell, as used in previous experiments,[1a,b] with a Pt counter and a calomel reference electrode. All potentials in this article are given versus the reversible hydrogen electrode (RHE).

Nanoparticle RDE electrodes were prepared by the solvothermal method described previously.[2b] $Ni(acetate)_2{\cdot}4H_2O$ and $[Pt(acac)_2]$ (acac = acetylacetonate) were the precursors for the PtNi nanoparticles and added in a proper ratio, to ensure a 1:1 PtNi alloy is formed. PtNi acid-treated and PtNi acid-treated/annealed nanoparticles with the average particle size of 5 nm were supported on high-surface-area carbon and their electrochemical properties were compared to Tanaka Pt/C with similar particle size (total metal content for all catalysts was 40%). The catalysts were deposited on 6 mm glassy carbon electrode and the loading in all cases was adjusted to be 12 $\mu g_{Pt}/cm_{disc}$.

Received: October 31, 2011
Revised: December 21, 2011
Published online: February 20, 2012

Keywords: adsorption · alloys · electrochemistry · nanoparticles · platinum

[1] a) V. R. Stamenkovic, B. Fowler, B. S. Mun, G. F. Wang, P. N. Ross, C. A. Lucas, N. M. Markovic, *Science* **2007**, *315*, 493 – 497; b) V. R. Stamenkovic, B. S. Mun, M. Arenz, K. J. J. Mayrhofer, C. A. Lucas, G. F. Wang, P. N. Ross, N. M. Markovic, *Nat. Mater.* **2007**, *6*, 241 – 247; c) V. R. Stamenkovic, B. S. Mun, K. J. J. Mayrhofer, P. N. Ross, N. M. Markovic, *J. Am. Chem. Soc.* **2006**, *128*, 8813 – 8819; d) I. E. L. Stephens, A. S. Bondarenko, F. J. Perez-Alonso, F. Calle-Vallejo, L. Bech, T. P. Johansson, A. K. Jepsen, R. Frydendal, B. P. Knudsen, J. Rossmeisl, I. Chorkendorff, *J. Am. Chem. Soc.* **2011**, *133*, 5485 – 5491.

[2] a) C. Wang, D. van der Vilet, K. C. Chang, H. D. You, D. Strmcnik, J. A. Schlueter, N. M. Markovic, V. R. Stamenkovic, *J. Phys. Chem. C* **2009**, *113*, 19365 – 19368; b) C. Wang, G. F. Wang, D. van der Vliet, K. C. Chang, N. M. Markovic, V. R. Stamenkovic, *Phys. Chem. Chem. Phys.* **2010**, *12*, 6933 – 6939; c) S. Chen, W. C. Sheng, N. Yabuuchi, P. J. Ferreira, L. F. Allard, Y. Shao-Horn, *J. Phys. Chem. C* **2009**, *113*, 1109 – 1125.

[3] a) B. Fowler, C. A. Lucas, A. Omer, G. Wang, V. R. Stamenkovic, N. M. Markovic, *Electrochim. Acta* **2008**, *53*, 6076 – 6080; b) S. Modak, S. Gangopadhyay, *Solid State Commun.* **1991**, *78*, 429 – 432.

[4] H. Schulenburg, J. Durst, E. Muller, A. Wokaun, G. G. Scherer, *J. Electroanal. Chem.* **2010**, *642*, 52 – 60.

[5] a) C. Wang, D. van der Vliet, K. L. More, N. J. Zaluzec, S. Peng, S. Sun, H. Daimon, G. Wang, J. Greeley, J. Pearson, A. P. Paulikas, G. Karapetrov, D. Strmcnik, N. M. Markovic, V. R. Stamenkovic, *Nano Lett.* **2011**, *11*, 919 – 926; b) P. Strasser, S. Koh, T. Anniyev, J. Greeley, K. More, C. F. Yu, Z. C. Liu, S. Kaya, D. Nordlund, H. Ogasawara, M. F. Toney, A. Nilsson, *Nat. Chem.* **2010**, *2*, 454 – 460; c) A. R. Malheiro, J. Perez, E. I. Santiago, H. M. Villullas, *J. Phys. Chem. C* **2010**, *114*, 20267 – 20271; d) C. Wang, M. Chi, D. Li, D. Strmcnik, D. van der Vliet, G. Wang, V. Komanicky, K.-C. Chang, A. P. Paulikas, D. Tripkovic, J. Pearson, K. L. More, N. M. Markovic, V. R. Stamenkovic, *J. Am. Chem. Soc.* **2011**, *133*, 14396 – 14403.

[6] S. Axnanda, K. D. Cummins, T. He, D. W. Goodman, M. P. Soriaga, *ChemPhysChem* **2010**, *11*, 1468 – 1475.

[7] a) A. Atli, M. Abon, J. C. Bertolini, *Surf. Sci.* **1993**, *287 – 288*, 110 – 113; b) J. C. Bertolini, B. Tardy, M. Abon, J. Billy, P. Delichère, J. Massardier, *Surf. Sci.* **1983**, *135*, 117 – 127; c) G. Chiarello, A. R. Marino, V. Formoso, A. Politano, *J. Chem. Phys.* **2011**, *134*, 224705.

[8] K. J. Andersson, F. Calle-Vallejo, J. Rossmeisl, L. Chorkendorff, *J. Am. Chem. Soc.* **2009**, *131*, 2404 – 2407.

[9] a) D. Strmcnik, D. Tripkovic, D. van der Vliet, V. Stamenkovic, N. M. Markovic, *Electrochem. Commun.* **2008**, *10*, 1602 – 1605; b) J. M. Orts, R. Gómez, J. M. Feliu, A. Aldaz, J. Clavilier, *Electrochim. Acta* **1994**, *39*, 1519 – 1524.

[10] a) B. Hammer, L. B. Hansen, J. K. Nørskov, *Phys. Rev. B* **1999**, *59*, 7413 – 7421;b) L. Bengtsson, *Phys. Rev. B* **1999**, *59*, 12301 – 12304;c) D. Vanderbilt, *Phys. Rev. B* **1990**, *41*, 7892 – 7895;d) G. Kresse, J. Furthmuller, *Comput. Mater. Sci.* **1996**, *6*, 15 – 50;e) F. Abild-Pedersen, J. Greeley, F. Studt, P. G. Moses, J. Rossmeisl, T. Munter, T. Bligaard, J. K. Nørskov, *Phys. Rev. Lett.* **2007**, *99*, 016105;f) D. Strmcnik, D. Tripkovic, D. van der Vliet, K. C. Chang, V. Komanicky, H. You, J. Greeley, V. Stamenkovic, N. M. Markovic, *J. Am. Chem. Soc.* **2008**, *130*, 15332 – 15339.

